Ab Initio Calculation of Structures and Properties of Halogenated General Anesthetics: Halothane and Sevoflurane

PEI TANG, IGOR ZUBRYZCKI, YAN XU

Department of Anesthesiology and Critical Care Medicine and Department of Pharmacology, University of Pittsburgh School of Medicine, W1358 Biomedical Science Tower, Pittsburgh, Pennsylvania 15261

Received 3 March 2000; accepted 26 September 2000

ABSTRACT: To correctly analyze the effects of general anesthetics on their potential targets by large-scale molecular simulation, the structural parameters and partial atomic charges of the anesthetics are of determinant importance. Geometric optimizations using the Hartree–Fock and the B3LYP density functional theory methods with the large 6-311+G(2d,p) basis set were performed to determine the structures and charge distributions of two halogenated anesthetics, 2-bromo-2-chloro-1,1,1-trifluoroethane (halothane) and fluoromethyl-2,2,2,-trifluoro-1-(trifluoromethyl) ethyl ether (sevoflurane). The calculated bond lengths and angles are within 3% of the corresponding experimental values reported for the similar molecular groups. Charges are assigned using the Mulliken population analysis and the electrostatic potential (ESP) based on the Merz–Kollman–Singh scheme. The atoms-in-molecules (AIM) theory is also used to assign the charges in halothane. The dipole moments calculated with the Mulliken population analysis and ESP for the structures optimized by B3LYP/6-311+(2d,p) were respectively 1.355 and 1.430 D for halothane and 2.255 and 2.315 D for sevoflurane. These are in excellent agreement with the experimental values of 1.41 and 2.33 D for halothane and sevoflurane, respectively. The calculated structures and partial charge distributions can be readily parameterized for molecular mechanics and molecular dynamics simulations involving these halogenated agents. J Comput Chem 22: 436–444, 2001

Keywords: *ab initio* calculation; B3LYP; electrostatic potential; general anesthetics; halothane; partial atomic charge; sevoflurane

Correspondence to: Yan Xu; e-mail: xuy@anes.upmc.edu

Contract/grant sponsor: National Institute of General Medical Sciences; contract/grant numbers: R01GM56257 (to P.T.) and R01GM49202 (to Y.X.)

Contract/grant sponsor: Pittsburgh Supercomputering Center (NIH National Center for Research Resources); contract/grant number: 2 P41 RR06009

Introduction

Computer-based molecular modeling is an indispensable tool for delineating detailed molecular interactions between drugs and their targets.[1–3] Particularly when low-affinity drugs with profound neurological effects are considered, critical issues often involve the identification of the sites at which the binding occurs and the structural and dynamic consequences of the binding. Examples of such low-affinity but neurologically active drugs are volatile general anesthetics. Despite the maturity of modern anesthesia practice, the molecular mechanisms of general anesthesia remain elusive. Recently, an increasing attention has been directed to the details of structural specificity of anesthetic binding on proteins.[4–9] In this regard, molecular modeling—complementary to experimental approaches—has the advantage of depicting not only the location, but also the nature of the interactions. The latter is important in the development of the theory of general anesthesia.[7] The concept of whether an interaction is specific or nonspecific depends both on the fitness of the drugs to the tertiary structures of the targets and on the forces and time constants involved in the interaction.

A class of clinically important general anesthetics is inhalational volatile anesthetics. These molecules are mostly halogenated compounds. A problem frequently encountered in using molecular dynamics (MD) simulation to study the effects of these drugs on protein structures and dynamics is the lack of a robust force field for the halogenated molecules. It is well known that when halogens are involved, many semiempirical calculations, though less time-consuming, fail to produce good predictions of the geometric parameters and electron densities for even the smallest molecules.[10] Reliable computational approach often requires *ab initio* calculation with sufficiently large basis sets.[11]

On the theoretical front, the new development of density-functional theory (DFT)[12–14] with consideration of various formulations of exchange and correlation functionals (both local and nonlocal) have brought *ab initio* calculations to a more accurate level. Particularly, the hybrid functionals, having a mixture of Hartree–Fock exchange and DFT exchange and correlation terms (e.g., B3LYP and B3PW91), have become state of the art in many recent applications. These new methods, combined with large basis sets, have brought halogenated molecules into the realm of accurate *ab initio* predictions. For example, recent *ab initio* calculations using B3LYP/6-31G* and B3PW91/6-311G(2d) have determined, among different conformers, the absolute configurations and predominant conformations of two fluorinated anesthetics, desflurane and 1,2,2,2-tetrafluoroethyl methyl ether.[15, 16]

We recently studied the different interactions of anesthetics and nonimmobilizers with a model transmembrane ion channel using nuclear magnetic resonance spectroscopy and photoaffinity labeling.[5, 6, 17] To further elucidate the molecular details of the drug effects on channel dynamics using large-scale MD simulation, a need has arisen for a better topology description of the anesthetics. Here we report the results of *ab initio* calculations of two halogenated volatile anesthetics, 2-bromo-2-chloro-1,1,1-trifluoroethane (halothane) and fluoromethyl-2,2,2,-trifluoro-1-(trifluoromethyl) ethyl ether (sevoflurane), using the Restricted Hartree–Fock (RHF) approach and the B3LYP hybrid DFT method. Large basis sets were used on the assumption that a more complete basis set will result in more accurate structural parameters and electrostatic potentials, permitting a better partial charge distribution assignment and reasonable prediction of experimental dipole moments. Halothane and sevoflurane (Fig. 1) were chosen for their popularity in clinical and experimental use and for the availability of their experimental dipole moment data.

Methods

All *ab initio* calculations were performed on the Cray-J90 computer at the Pittsburgh Supercomputing Center using the Gaussian 98 program.[18] Two series of calculations were carried out using the Restricted Hartree–Fock and the hybrid B3LYP DFT methods, respectively. The B3LYP method uses Becke's three-parameter functional[14] with the nonlocal correlation term provided by the Lee–Yang–Parr expression.[19] The large 6-311+G(2d,p) basis set[20, 21] was used with both methods for both molecules. The following convergence criteria were imposed (in atomic units): maximum force = 0.000450, RMS force = 0.000300, maximum displacement = 0.001800, and RMS displacement = 0.001200.

When the convergence at B3LYP/6-311+G(2d,p) level became a problem, a multiple-step approach was taken by successively increasing the size of the basis sets and using the optimized geometries with the smaller sets as the inputs for the calculations with the larger sets. Geometry optimization of

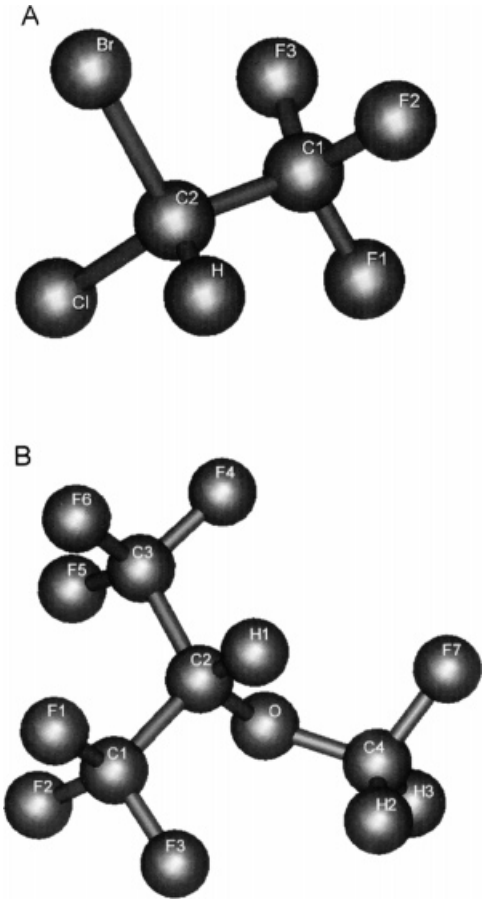

FIGURE 1. Molecular structures of halothane (A) and sevoflurane (B) and the labeling convention used in the text and tables. (Molecules are not drawn to the same scale.)

sevoflurane was done in the following order, with the output of each run as the input of the subsequent run: HF/6-311+G(2d,p), B3LYP/6-31G(d,p), B3LYP/6-311G(2d,p), and B3LYP/6-311+G(2d,p).

The charge assignments of the geometry-optimized structures and dipole moments were derived from the Mulliken population analysis[22] and the electrostatic potential (ESP) using the Merz–Kollman–Singh (MKS) scheme.[23] Because halothane contains two heavy halogen atoms of the third and forth row (Cl and Br) whose Van der Waals radii are more charge dependent, the ESP-derived charges often vary with the ESP fitting schemes. We, therefore, also used the atoms-in-molecule (AIM) theory[24] to calculate the charge distribution in halothane. In addition, the highest occupied molecular orbital (HOMO) and the lowest unoccupied molecular orbital (LUMO) were evaluated using Gaussian. The gOpenMol program (http://laaksonen.csc.fi/gopenmol) was used for the final rendering of the calculated structures, partial atomic charge distribution, HOMO, and LUMO.

Results

The Cartesian coordinates of the atoms in the standard orientation of the geometry-optimized halothane and sevoflurane molecules are given in Tables I and II, respectively. The atomic centers are labeled as shown in Figure 1. The bond lengths and bond angles (including the torsion angles) are listed in Tables III and IV, respectively. Also listed in Tables III and IV are averaged values of corresponding bond lengths or bond angles obtained experimentally for similar molecular groups in the gas phase.[25] Partial atomic charges, assigned based on the Mulliken population analysis, are listed in Tables V and VI for halothane and sevoflurane, respectively. In Figure 2, the ESP from the B3LYP/6-311+G(2d,p) calculations is mapped onto the electron density

TABLE I.
Cartesian Coordinates (in Angstroms) of Atoms in the Standard Orientation of Halothane.

Atomic Center	Atomic Number	HF/6-311+G(2d,p)			B3LYP/6-311+G(2d,p)		
		X	Y	Z	X	Y	Z
C1	6	1.221069	−0.556414	0.000300	1.221791	−0.568805	0.000637
F1	9	2.381550	−0.122556	−0.430345	2.418548	−0.142844	−0.440538
F2	9	1.053796	−1.768934	−0.468632	1.034864	−1.809133	−0.479791
F3	9	1.263610	−0.618260	1.302009	1.267031	−0.634263	1.332415
C2	6	0.112186	0.354676	−0.511291	0.119931	0.363511	−0.515590
Br	35	−1.622322	−0.307253	0.013683	−1.644207	−0.296886	0.013135
Cl	17	0.373559	2.012084	0.032002	0.404273	2.032007	0.030635
H	1	0.140636	0.346586	−1.584292	0.140282	0.354804	−1.599565

TABLE II.
Cartesian Coordinates (in Angstroms) of Atoms in the Standard Orientation of Sevoflurane.

Atomic Center	Atomic Number	HF/6-311+G(2d,p)			B3LYP/6-311+G(2d,p)		
		X	Y	Z	X	Y	Z
C1	6	1.047304	−1.028009	−0.076523	0.965884	−1.108842	−0.077392
F1	9	1.958603	−0.802282	−0.990055	−0.140326	−0.047479	−0.215119
F2	9	1.614434	−0.962188	1.097641	−1.146688	−0.290483	0.739467
F3	9	0.611992	−2.259732	−0.244618	1.910180	−0.956700	−1.016920
C2	6	−0.131077	−0.068017	−0.218808	1.554780	−1.092362	1.120745
H1	1	−0.488265	−0.149536	−1.237395	0.418076	−2.332257	−0.247247
C3	6	0.233301	1.398330	−0.004482	0.351093	1.395390	−0.007020
F4	9	−0.822598	2.141951	−0.215738	−0.664322	2.245263	−0.209023
F5	9	0.660409	1.631944	1.208355	0.824444	1.598856	1.227124
F6	9	1.166489	1.773794	−0.847476	1.322700	1.698081	−0.884854
O	8	−1.100060	−0.397626	0.711809	−0.517988	−0.100126	−1.239031
C4	6	−2.208008	−1.070616	0.259195	−2.291675	−0.930537	0.274037
F7	9	−2.923890	−0.279088	−0.568645	−2.910387	−1.119800	1.148222
H2	1	−2.806201	−1.298703	1.124604	−2.993297	−0.101504	−0.588904
H3	1	−1.943129	−1.960465	−0.293156	−2.061025	−1.841791	−0.280249

TABLE III.
Bond Lengths of Geometry-Optimized Halothane and Sevoflurane.

Molecules						
Halothane Length (Å)			Sevoflurane Length (Å)			
Bond	HF	B3LYP	Bond	HF	B3LYP	Experimental[a] (Å)
C1—F1	1.311	1.345	C1—F1	1.310	1.341	
C1—F2	1.310	1.343	C1—F2	1.306	1.335	
C1—F3	1.304	1.334	C1—F3	1.317	1.351	1.340 ± 0.019 (MW, ED)
			C3—F4	1.309	1.340	
			C3—F5	1.307	1.337	
			C3—F6	1.312	1.344	
C1—C2	1.523	1.533	C1—C2	1.526	1.539	1.526 ± 0.028 (MW, ED)
			C3—C2	1.526	1.538	
			C2—O	1.383	1.408	1.410 ± 0.026 (MW, ED)
			O—C4	1.373	1.392	
			C4—F7	1.351	1.387	1.390 (ED)
			C2—H1	1.083	1.093	
			C4—H2	1.076	1.088	1.095 ± 0.011 (MW, ED)
			C4—H3	1.080	1.091	
C2—H	1.073	1.084				1.094 ± 0.001 (MW, ED, IR)
C2—Br	1.929	1.957				1.928 ± 0.006 (MW, ED)
C2—Cl	1.764	1.779				1.769 ± 0.012 (MW, ED, IR)

[a] Averaged bond lengths (mean ± SD) of similar molecular groups listed in the CRC Handbook of Chemistry and Physics, pp. 9–41, 1994. Experimental methods include microwave spectroscopy (MW), electron diffraction (ED), and infrared spectroscopy (IR).

TABLE IV.
Bond and Torsion Angles of Geometry-Optimized Halothane and Sevoflurane.

Halothane			Sevoflurane			
	Angles (deg)			Angles (deg)		Experimental[a]
Bonds	HF	B3LYP	Bonds	HF	B3LYP	(deg)
F1—C1—F2	107.6	107.4	F1—C1—F2	108.4	108.5	
F1—C1—F3	108.3	108.2	F1—C1—F3	107.6	107.5	
F2—C1—F3	108.5	108.4	F2—C1—F3	107.5	107.6	108.3 (MW)
			F4—C3—F5	108.2	108.1	
			F4—C3—F6	107.9	107.9	
			F5—C3—F6	108.2	108.2	
F1—C1—C2	109.6	109.7	F1—C1—C2	111.3	111.4	
F2—C1—C2	109.9	109.9	F2—C1—C2	112.8	112.9	
F3—C1—C2	112.8	113.0	F3—C1—C2	108.7	108.8	110.2 ± 0.6 (MW, ED)
			F4—C3—C2	109.3	109.4	
			F5—C3—C2	112.3	112.4	
			F6—C3—C2	110.8	110.7	
			H2—C4—H3	111.9	112.5	109.8 ± 1.2 (MW, ED)
C1—C2—Cl	110.5	110.6				110.2 ± 0.8 (MW, ED)
C1—C2—H	108.2	108.6				111.8 ± 1.7 (ED)
Br—C2—Cl	111.8	112.2				111.5 ± 0.7 (MW, ED)
Cl—C2—H	108.1	108.2				109.6 ± 2.8 (ED)
C1—C2—Br	111.0	110.6				
Br—C2—H	107.0	106.5				
			C1—C2—C3	114.0	113.9	
			C3—C2—H1	106.4	106.4	
			C1—C2—H1	107.2	107.4	
			H1—C2—O	112.6	112.3	
			C2—O—C4	117.4	116.1	
			O—C4—F7	110.0	110.4	
			O—C4—H2	106.7	106.2	
			O—C4—H3	112.0	112.3	
			H2—C4—F7	108.8	108.4	
			H3—C4—F7	107.4	106.9	
			F1—C1—C2—O	176.4	176.6	
			F4—C3—C2—O	−62.2	−61.5	
			C1—C2—O—C4	−103.4	−100.9	
			C3—C2—O—C4	132.4	135.2	
			H1—C2—O—C4	15.4	18.6	
			C2—O—C4—F7	−66.1	−67.8	
F1—C1—C2—Br	176.7	176.3				
F1—C1—C2—Cl	−58.6	−58.7				
F1—C1—C2—H	59.5	59.8				
F2—C1—C2—Br	58.6	58.4				
F2—C1—C2—Cl	−176.7	−176.6				
F2—C1—C2—H	−58.5	−58.1				
F3—C1—C2—Br	−62.5	−62.9				
F3—C1—C2—Cl	62.2	62.1				
F3—C1—C2—H	−179.6	−179.4				

[a] See the note in Table III.

TABLE V.
Assignment of Partial Atomic Charges in Halothane.

Atomic Center	Mulliken Partial Atomic Charges		AIM Charges
	HF	B3LYP	
C1	0.9593	0.7269	1.7762
F1	−0.3878	−0.2930	−0.6167
F2	−0.3765	−0.2866	−0.6196
F3	−0.3649	−0.2767	−0.6231
C2	0.0177	−0.1058	0.0760
Br	0.0049	0.0279	−0.0100
Cl	−0.0428	0.0140	−0.1280
H	0.1901	0.1934	0.1349

TABLE VI.
Assignment of Partial Atomic Charges in Sevoflurane.

Atomic Center	Mulliken Partial Atomic Charges	
	HF	B3LYP
C1	1.3575	1.0405
F1	−0.3989	−0.2996
F2	−0.4044	−0.3020
F3	−0.4171	−0.3190
C2	−0.3000	−0.3352
H1	0.1683	0.1649
C3	1.2972	1.0034
F4	−0.4014	−0.3024
F5	−0.4016	−0.3005
F6	−0.4090	−0.3092
O	−0.4430	−0.3217
C4	0.4673	0.2984
F7	−0.3744	−0.2988
H2	0.1316	0.1425
H3	0.1279	0.1387

surface (at the contour of 0.1 a.u.) for the geometry-optimized halothane and sevoflurane. The HOMOs and LUMOs are plotted in Figure 3. The three components of the dipole moments and total dipole moments, derived from the Mulliken population analysis and ESP using the MKS scheme, are tabulated in Table VII for geometry-optimized halothane and sevoflurane. The experimental values are also listed for comparison.

Discussion

Although many Gaussian basis sets are suited for *ab initio* calculation of mono-halogenated molecules, the results presented here suggest that the selection of the larger basis sets, such as 6-311+G(2d,p), works reasonably well for some poly-halogenated molecules. The geometric parameters listed in Tables III and IV demonstrate that the calculated bond lengths and bond angles are within 3% of the averaged experimental values of similar molecular groups. For both halothane and sevoflurane, the B3LYP-level chemistry provides better prediction of the geometric parameters than does the HF level, particularly the C—F bond lengths. It should be noted that even within the same CF_3 group, the C—F bond lengths and angles are not equal due to the overall asymmetry of the molecules. The calculated C—C bond lengths are very close to the experimental values in the gas phase. For all bond lengths and bond angles, some small differences from the experimental values are expected considering the wide range of molecular structures being included in the calculation of the experimental averages in Tables III and IV. Overall, the excellent agreement between calculated and experimental results suggests that the calculated geometric parameters are rather accurate.

Given the reasonable geometric configurations, it is often desirable to assign charges to the atomic centers, considering the widespread use of the partial atomic charge model in molecular mechanics and molecular dynamics simulations. A popular assignment scheme is based on the Mulliken population analysis (see Tables V and VI). For halothane, although the C1 atomic center adopts a positive charge, the CF_3 moiety is slightly electronegative ($-0.1698e$ and $-0.1294e$ at the HF and B3LYP level calculations, respectively) due to the strong electronegativity of fluorine atoms. The partial atomic charge distribution in sevoflurane is slightly more complicated. While the fluorine centers in the two CF_3 groups are more negatively charged than the values in halothane from the corresponding method of calculation, the CF_3 groups are electropositive in sevoflurane. The middle segment of the molecule surrounding the C2—O bond is more electronegative. It should be noted that partial atomic charges are not experimentally observable quantities, and their values often depend on the partitioning scheme. The Mulliken population analysis assigns the diagonal components of the electron density matrix to the atoms on which the corresponding orbital is located and equally divides the off-diagonal components to the atoms of the overlapping populations. This partitioning scheme is known to be susceptible to errors, particularly when

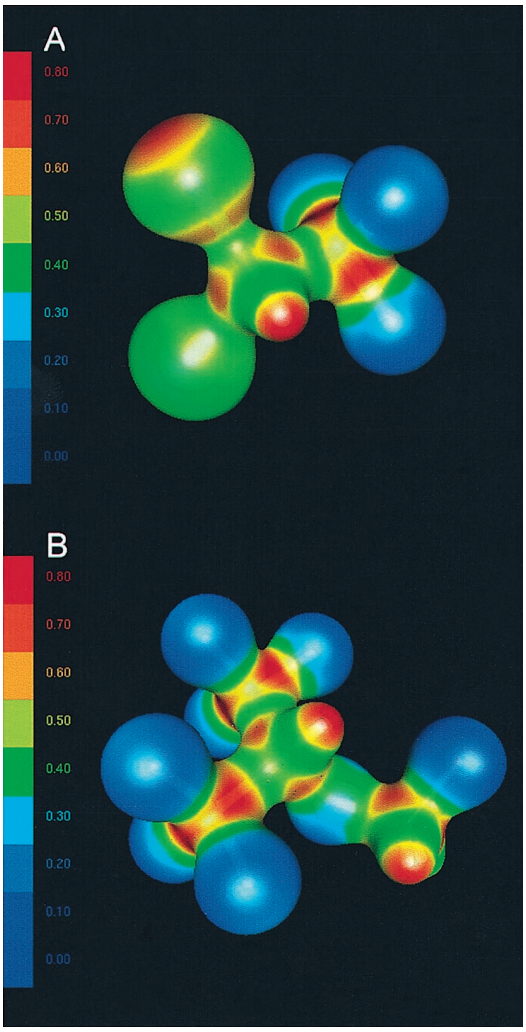

FIGURE 2. Electrostatic potential (ESP) mapped onto the electron density surface (at a contour of 0.1 au) for halothane (A) and sevoflurane (B). The color bars are in atomic unit. The surfaces are made slightly transparent so that the skeleton of the molecular structures can be visualized. (Molecules are in the same orientation as shown in Fig. 1, but are not drawn to the same scale.)

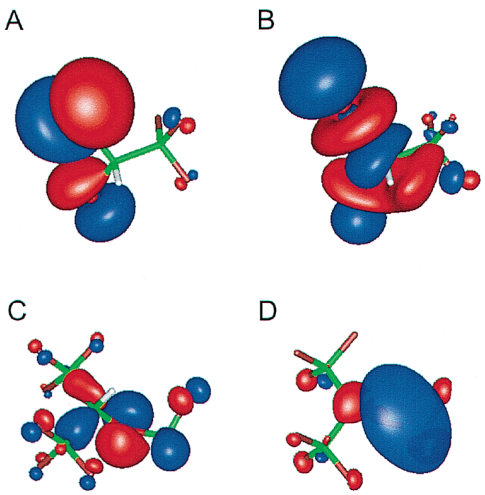

FIGURE 3. The highest occupied molecular orbital (HOMO) and the lowest unoccupied molecular orbital (LUMO) for halothane (A and B, respectively) and sevoflurane (C and D, respectively). The red contour indicates the negative part of the wave function and the blue the positive part of the wave function. (Molecules are in the same orientation as shown in Fig. 1, but are not drawn to the same scale.)

large diffuse components are involved. Thus, when the objective is to determine interactions between molecules, a scheme based on the properties of intermolecular interactions, such as electrostatic potential, is probably more appropriate. Indeed, at the B3LYP level, the ESP-derived charge distribution based on the MKS scheme gives better predictions of the electric dipole moments (Table VII). Two other ESP-based schemes, the CHELP procedure of Chirlian and Francl[26] and the CHELPG algorithm of Berneman and Wiberg,[27] also yield comparable dipole results (data not shown). As indicated in Table VII, the predicted dipole moments are in excellent agreement with the experimental value of 1.41 D for halothane[28] and 2.33 D for sevoflurane (courtesy of Dr. Dale Brugh of Ohio Wesleyan University and Dr. Richard Suenram of NIST).

Although ESP-based schemes are widely used to derive charges for popular force fields such as AMBER, it should be noted that most ESP-based schemes suffer from the drawback that partial atomic charges are critically dependent on the surface grids used for fitting the ESP. Because the most relevant surfaces for intermolecular interaction are those on or very near the van der Waals surface of the molecules, it follows that the ESP-derived charges vary with the van der Waals radii of the atoms in the molecule. Hence, a "good" set of van der Waals radii can only be estimated either based on the partial atomic charges derived from other methods or by assigning charges and van der Waals radii iteratively until certain observable properties are met. This can lead to rather large variation in partial atomic charges for molecules having heavy halogen atoms such as Br and Cl, because the van der Waals radii of these heavy halogens

TABLE VII.
Dipole Moments of Halothane and Sevoflurane.

Dipole Moments (Debye)	Halothane				Sevoflurane			
	HF		B3LYP		HF		B3LYP	
	Mulliken	ESP	Mulliken	ESP	Mulliken	ESP	Mulliken	ESP
D_x	−0.530	−0.464	−0.589	−0.513	−1.330	−1.367	−1.283	−1.326
D_y	0.337	0.329	0.398	0.393	−2.045	−2.084	−1.813	−1.853
D_z	−1.273	−1.390	−1.153	−1.275	−0.510	−0.534	−0.387	−0.408
D_{Total}	1.419	1.502	1.355	1.430	2.492	2.548	2.255	2.315
$D_{Experimental}$	1.41[a]				2.33[b]			

[a] Ref. 28.
[b] Unpublished result, courtesy of Drs. Dale Brugh and Richard Suenram.

are often charge dependent. For example, when the default MKS van der Waals radii are inputted to the CHELPG schemes, the partial atomic charges on Br and Cl are $-0.035e$ and $0.000e$, respectively, compared to $+0.045e$ and $+0.051e$ obtained with the default CHELPG radii. Interestingly, the dipole moments calculated from the two radii sets are not greatly different (1.45 D vs. 1.49 D).

An alternative approach to minimizing the arbitrariness in assigning charges to heavy halogens is to use a method that is insensitive to the calculation method and basis set. Electron density partitioning based on the AIM theory proves to be robust in this regard.[29–35] As shown in Table V, the AIM-derived charges at attractors centered on the F atoms are more electronegative than the corresponding Mulliken charges but seem to be more consistent with the strong electron-pulling capability of fluorine. Indeed, based on the AIM partitioning, the total numbers of electrons belonging to C1, three F's, C2, Br, Cl, and H, are roughly 4.2, 9.6, 5.9, 35.0, 17.1, and 0.9, respectively. The AIM-derived dipole moment for halothane is 1.442 D.

Structural calculation of halothane molecule has been performed previously[36] using energy minimization within the Car–Parrinello scheme of the density functional theory.[37] The Vanderbilt supersoft pseudopotentials[38] were applied along with the local density approximation (LDA) approach for the exchange-correlation energy term. In that calculation, the bond lengths for halothane were found nearly the same as the corresponding B3LYP values in Table III, and the bond angles differed from the values listed in Table IV by about ±2°. These differences are considered small, and can be attributed to the different methods used for the calculations. The major difference is the partial atomic charges, which, as discussed above, can be attributed to the different schemes used for the assignment. Most noticeable is that the previous assignment sets both methyl groups to electroneutral, whereas all of the schemes used in this study yielded net electronegativity associated with the —CF_3 moiety. The dipole moment from the previous calculation ranged from 1.83 to 2.20 D, which is about 30–56% larger than the experimental value.

The correct parameterization of the structures and properties of anesthetics is critical to the quality of further molecular mechanisms or molecular dynamics simulations that involve these anesthetic molecules. A compromised force field, including the charges, bond lengths, and bond angles, could lead to incorrect simulation conclusions regarding the effects of these halogenated anesthetics on their potential targets. As have been stressed by other investigators,[39] one of the critical parameters is the partial atomic charge. Because different schemes can produce rather large variations in charge distribution in the same optimized structure, it is always advisable to choose a scheme that is either invariant to the calculation method and basis set (such as AIM) or consistent with certain molecular properties (such as electric multiples) that can be verified experimentally.

Acknowledgments

The authors would like to thank Dr. David Pratt for stimulating discussion, Dr. Dale Brugh and Dr. Richard Suenram for sharing their sevoflurane data, and Dr. Kenneth D. Jordan, Dr. Lindsey J. Munro, and Dr. Fernando D. Vila for stimulating discussion and the help with the Gaussian98 program.

References

1. Zubrzycki, I. Z.; Xu, Y.; Madrid, M.; Tang, P. J Chem Phys 2000, 112, 3437.
2. Woska, A. B.; Klein, M. L.; Scharf, D. Toxicol Lett 1998, 100–101, 377.
3. Forrest, L. R.; Kukol, A.; Arkin, I. T.; Tieleman, D. P.; Sansom, M. S. Biophys J 2000, 78, 55.
4. Xu, Y.; Seto, T.; Tang, P.; Firestone, L. Biophys J 2000, 78, 746.
5. Tang, P.; Hu, J.; Liachenko, S.; Xu, Y. Biophys J 1999, 77, 739.
6. Tang, P.; Simplaceanu, V.; Xu, Y. Biophys J 1999, 76, 2346.
7. Xu, Y.; Tang, P.; Liachenko, S. Toxicol Lett 1998, 100–101, 347.
8. Johansson, J. S.; Scharf, D.; Davies, L. A.; Reddy, K. S.; Eckenhoff, R. G. Biophys J 2000, 78, 982.
9. Eckenhoff, R. G.; Johansson, J. S. Pharmacol Rev 1997, 49, 343.
10. Stewart, J. J. J Comput Aided Mol Design 1990, 4, 1.
11. Leach, A. R. Molecular Modelling: Principals and Applications; Longman: Essex, 1996.
12. Becke, A. D. J Chem Phys 1992, 96, 2155.
13. Becke, A. D. J Chem Phys 1992, 97, 9173.
14. Becke, A. D. J Chem Phys 1993, 98, 5648.
15. Polavarapu, P. L.; Zhao, C. X.; Cholli, A. L.; Vernice, G. G. J Phys Chem B 1999, 103, 6127.
16. Polavarapu, P. L.; Zhao, C. X.; Ramig, K. Tetrahedron-Asymmetry 1999, 10, 1099.
17. Tang, P.; Eckenhoff, R. G.; Xu, Y. Biophys J 2000, 78, 1804.
18. Frisch, M. J.; Trucks, G. W.; Schlegel, H. B.; Scuseria, G. E.; Robb, M. A.; Cheeseman, J. R.; Zakrzewski, V. G.; Montgomery, Jr., J. A.; Stratmann, R. E.; Burant, J. C.; Dapprich, S.; Millam, J. M.; Daniels, A. D.; Kudin, K. N.; Strain, M. C.; Farkas, O.; Tomasi, J.; Barone, V.; Cossi, M.; Cammi, R.; Mennucci, B.; Pomelli, C.; Adamo, C.; Clifford, S.; Ochterski, J.; Petersson, G. A.; Ayala, P. Y.; Cui, Q.; Morokuma, K.; Malick, D. K.; Rabuck, A. D.; Raghavachari, K.; Foresman, J. B.; Cioslowski, J.; Ortiz, J. V.; Stefanov, B. B.; Liu, G.; Liashenko, A.; Piskorz, P.; Komaromi, I.; Gomperts, R.; Martin, R. L.; Fox, D. J.; Keith, T.; Al-Laham, M. A.; Peng, C. Y.; Nanayakkara, A.; Gonzalez, C.; Challacombe, M.; Gill, P. M. W.; Johnson, B.; Chen, W.; Wong, M. W.; Andres, J. L.; Gonzalez, C.; Head-Gordon, M.; Replogle, E. S.; Pople, J. A. Gaussian 98; Gaussian, Inc.: Pittsburgh, PA, 1998.
19. Lee, C.; Yang, W.; Parr, R. G. Phys Rev B 1988, 785.
20. Krishnan, R.; Binkley, J. S.; Seeger, R.; Pople, J. A. J Chem Phys 1980, 72, 650.
21. McLean, A. D.; CHandler, G. S. J Chem Phys 1980, 72, 5639.
22. Mulliken, R. S. J Chem Phys 1955, 23, 1833.
23. Besler, B. H.; Merz, K. M.; Kollman, P. A. J Comput Chem 1990, 11, 431.
24. Bader, R. F. Atoms in Molecules: A Quantum Theory; Oxford University Press: Oxford, 1990.
25. The CRC Handbook of Chemistry and Physics; Lide, D. R.; Frederikse, H. P. R., Eds.; CRC Press, Inc.: Boca Raton, FL, 1994, 74th ed.
26. Chirlian, L. E.; Francl, M. M. J Comput Chem 1987, 8, 894.
27. Breneman, C. M.; Wiberg, K. B. J Comput Chem 1990, 11, 361.
28. Fenclova, D.; Dohnal, V. J Chem Therm 1990, 22, 219.
29. Stefanov, B. B.; Cioslowski, J. J Comput Chem 1995, 16, 1394.
30. Cioslowski, J.; Stefanov, B. B. Mol Phys 1995, 84, 707.
31. Cioslowski, J.; Nanayakkara, A. Chem Phys Lett 1994, 219, 151.
32. Cioslowski, J.; Nanayakkara, A. J Am Chem Soc 1993, 115, 11213.
33. Cioslowski, J.; Nanayakkara, A.; Challacombe, M. Chem Phys Lett 1993, 203, 137.
34. Cioslowski, J. Chem Phys Lett 1992, 194, 73.
35. Cioslowski, J.; Surjan, P. R. J Mol Struct (Theochem) 1992, 87, 9.
36. Scharf, D.; Laasonen, K. Chem Phys Lett 1996, 258, 276.
37. Car, R.; Parrinello, M. Phys Rev Lett 1985, 55, 2471.
38. Vanderbilt, D. Phys Rev B 1990, 41, 7892.
39. Trudell, J. R.; Bertaccini, E. Toxicol Lett 1998, 100–101, 413.